Human Molecular Genetics, 2007, Vol. 16, No. 22 **2720–2728**
doi:10.1093/hmg/ddm226
Advance Access published on August 28, 2007

Familial amyotrophic lateral sclerosis-linked SOD1 mutants perturb fast axonal transport to reduce axonal mitochondria content

Kurt J. De Vos[1,2,*†], Anna L. Chapman[2,†], Maria E. Tennant[1,†], Catherine Manser[1,†], Elizabeth L. Tudor[1], Kwok-Fai Lau[3], Janet Brownlees[1], Steven Ackerley[1], Pamela J. Shaw[2], Declan M. McLoughlin[1], Christopher E. Shaw[1], P. Nigel Leigh[1], Christopher C.J. Miller[1,§] and Andrew J. Grierson[2,§]

[1]MRC Centre for Neurodegeneration Research, Institute of Psychiatry, King's College London, Denmark Hill, London SE5 8AF, UK, [2]Academic Unit of Neurology, School of Medicine and Biochemical Sciences, University of Sheffield, Sheffield S10 2RX, UK and [3]Department of Biochemistry, The Chinese University of Hong Kong, Shatin, NT, Hong Kong

Received July 23, 2007; Revised and Accepted August 14, 2007

Amyotrophic lateral sclerosis (ALS) is a late-onset neurological disorder characterized by death of motoneurons. Mutations in Cu/Zn superoxide dismutase-1 (SOD1) cause familial ALS but the mechanisms whereby they induce disease are not fully understood. Here, we use time-lapse microscopy to monitor for the first time the effect of mutant SOD1 on fast axonal transport (FAT) of bona fide cargoes in living neurons. We analyzed FAT of mitochondria that are a known target for damage by mutant SOD1 and also of membrane-bound organelles (MBOs) using EGFP-tagged amyloid precursor protein as a marker. We studied FAT in motor neurons derived from SOD1^{G93A} transgenic mice that are a model of ALS and also in cortical neurons transfected with SOD1^{G93A} and three further ALS-associated SOD1 mutants. We find that mutant SOD1 damages transport of both mitochondria and MBOs, and that the precise details of this damage are cargo-specific. Thus, mutant SOD1 reduces transport of MBOs in both anterograde and retrograde directions, whereas mitochondrial transport is selectively reduced in the anterograde direction. Analyses of the characteristics of mitochondrial FAT revealed that reduced anterograde movement involved defects in anterograde motor function. The selective inhibition of anterograde mitochondrial FAT enhanced their net retrograde movement to deplete mitochondria in axons. Mitochondria in mutant SOD1 expressing cells also displayed features of damage. Together, such changes to mitochondrial function and distribution are likely to compromise axonal function. These alterations represent some of the earliest pathological features so far reported in neurons of mutant SOD1 transgenic mice.

INTRODUCTION

Transport of protein and organelle cargoes to their correct destinations is essential for cellular function. Neurons are especially dependent upon the transport process because they are polarized and contain long processes through which cargoes have to be moved. Cytoskeletal and some other proteins are transported by slow axonal transport at an overall rate of about 1 mm/day. By contrast, membrane-bound organelles (MBOs) such as vesicles that contain a variety of proteins needed for axonal and synaptic function are transported to their destination by fast axonal transport (FAT) at rates of

*To whom correspondence should be addressed at: MRC Centre for Neurodegeneration Research, Department of Neuroscience PO37, The Institute of Psychiatry, King's College London, De Crespigny Park, Denmark Hill, London SE5 8AF, UK. Tel: +44 2078480393; Fax: +44 2077080017; Email: kurt.devos@iop.kcl.ac.uk
† and § These authors contributed equally to this work.

about 1μm/s (1,2). Mitochondria are transported by FAT, but in contrast to MBOs their transport involves prolonged pausing and frequent reversal of direction; such saltatory movement is believed to underlie the uniform distribution of mitochondria that is observed in axons (3,4). The importance of axonal transport for neuronal function and survival is highlighted by the fact that mutations in genes encoding molecular motors that drive axonal transport, or motor-associated proteins, cause some human neurodegenerative diseases (5,6).

Amyotrophic lateral sclerosis (ALS) is a neurodegenerative disorder that involves selective death of motoneurons. Some forms of ALS are familial and mutations in the antioxidant enzyme Cu/Zn superoxide dismutase-1 (SOD1) account for roughly 20% of these familial cases. Over 100 different SOD1 mutations are associated with ALS and although the mechanisms by which these mutants induce ALS are not properly understood, it is generally agreed that they have acquired one or more toxic properties (reviewed in 7).

Several mechanisms of mutant SOD1 toxicity to motoneurons have been proposed including oxidative stress, protein aggregation, mitochondrial dysfunction, excitotoxicity and impaired axonal transport (8). However, one of the earliest pathological features of mutant SOD1 transgenic mice is a reduction in slow axonal transport of cytoskeletal components (9,10), and disruption in retrograde transport of exogenously applied tetanus toxin fragments is seen in mutant SOD1 expressing motoneurons (11). Thus, compromised transport of selected cargoes may be an important component of mutant SOD1 toxicity.

Here, we have used live time-lapse microscopy to directly quantify the effect of mutant SOD1 on FAT in motoneurons and cortical neurons. We analyzed movement of mitochondria, which are a target of mutant SOD1, and the amyloid precursor protein (APP), a type-1 membrane-spanning protein that is widely used as a marker for axonal transport of MBOs (12–16). We find that mutant SOD1 perturbs transport of both mitochondria and APP-containing MBOs (MBO^{APP}) but that the nature of this damage is different for each cargo. Thus, our studies are the first to describe the effect of mutant SOD1 on FAT of defined bona fide axonal cargoes in living neurons, and as such provide novel insights into mutant SOD1 toxicity in ALS.

RESULTS

Mutant SOD1 disrupts FAT

To dissect the effect of mutant SOD1 on FAT, we quantified the overall transport of mitochondria and MBO^{APP} in axons of transgenic motoneurons and/or transfected rat cortical neurons from time-lapse recordings. Mitochondria were visualized either by use of MitoTracker CMXROS or by transfection of DsRed-Mito, and MBO^{APP} by transfection of EGFP-tagged APP (APP-EGFP).

We first studied axonal transport of mitochondria in motoneurons derived from transgenic mice expressing human $SOD1^{G93A}$ or wild type human SOD1 ($SOD1^{wt}$) and non-transgenic (ntg) littermates. Overall transport of mitochondria was analyzed by calculating the distance between the position of individual mitochondria at the start and end of time-lapse recordings and dividing by the time elapsed. This yielded an overall velocity of transport for each mitochondrion that includes anterograde and retrograde movements and stationary periods. Mitochondria were subsequently classified as motile (velocity > 0.1 μm/s) or stationary (velocity ≤ 0.1 μm/s).

In ntg and $SOD1^{wt}$ motoneurons ~35% of mitochondria were motile, and their anterograde and retrograde transport was balanced (Fig. 1). The number of motile mitochondria in $SOD1^{G93A}$ motoneurons did not differ significantly from those in ntg or $SOD1^{wt}$ neurons (Fig. 1Ba). However, in $SOD1^{G93A}$ motoneurons the number of retrograde mitochondria was increased by ~80%, and concurrently the fraction of anterograde mitochondria decreased. Consequently, the balance of transport was disturbed (Fig. 1Bb and c; retrograde > anterograde, $P < 0.001$, *t*-test).

To determine if this shift toward net retrograde movement of mitochondria was unique to $SOD1^{G93A}$, we expressed $SOD1^{G93A}$ and three more ALS-linked SOD1 mutants with different biochemical and disease-associated properties (7,17) ($SOD1^{A4V,\ G37R\ and\ G85R}$) in rat cortical neurons and monitored mitochondrial movement by time-lapse microscopy. To identify transfected neurons we tagged SOD1 with EGFP. All EGFP-tagged SOD1s (EGFP-SOD1) were expressed as full-length protein in neurons and were functionally indistinguishable from untagged SOD1 (Supplementary Material, Fig. S1).

In EGFP (control) and EGFP-$SOD1^{wt}$ transfected rat cortical neurons the number of motile mitochondria was similar to that in motoneurons, but significantly more motile mitochondria moved anterogradely than retrogradely in the cortical neurons (Fig. 1C). Axonal transport of mitochondria is known to alter developmentally and in response to metabolic demands (3,4). Net anterograde movement of mitochondria is thus clearly required for proper cellular function and a balanced distribution in axons of the 7–8 day rat cortical neurons utilized here. Expression of mutant SOD1s did not alter the number of motile mitochondria as compared to EGFP or EGFP-$SOD1^{wt}$ transfected neurons but as was the case in $SOD1^{G93A}$ motoneurons, all mutant SOD1s induced a significant increase in retrograde mitochondria and a corresponding decrease in anterograde movement (Fig. 1C). Thus, all mutant SOD1s tested disturbed FAT of mitochondria similarly.

We next analyzed the effects of mutant SOD1 on FAT of MBOs using APP-EGFP as a marker (MBO^{APP}). MBO^{APP} comprised elongated structures ranging from 1.66 to 10.47μm in length (3.55 ± 1.58 μm; mean ± SD) and smaller MBO^{APP} vesicles (0.54–1.15 μm in diameter; 0.75 ± 0.10 μm). These MBO^{APP} corresponded closely to the APP-YFP elongated tubules and vesicles that have been described previously (12,14).

We co-transfected rat cortical neurons with APP-EGFP and either vector expressing *Escherichia coli* chloramphenicol acetyltransferase (CAT) as a control, $SOD1^{wt}$, $SOD1^{G37R,\ G93A,\ G85R\ or\ A4V}$ and monitored movement of MBO^{APP}. To ensure that all APP-EGFP transfected cells studied also expressed transfected SOD1, the cells were fixed following analysis and stained for human SOD1. As a measure of overall transport, we determined the total distance MBO^{APP} moved per minute of observation time from

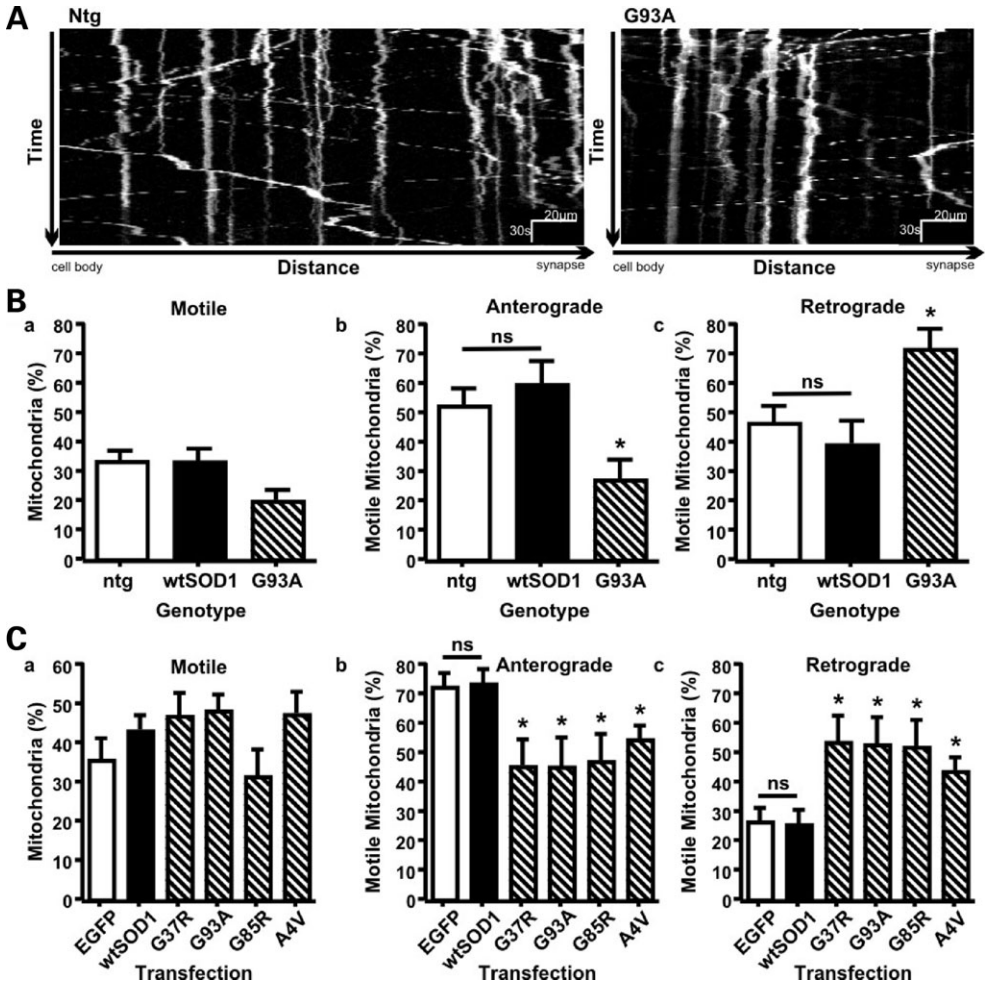

Figure 1. Mutant SOD1 enhances net retrograde FAT of mitochondria. Transport of mitochondria was recorded in time-lapse (3 s interval for 10–20 min) in ntg (open bar), SOD1^{wt} (closed bar), and SOD1^{G93A} (hatched bar) transgenic motoneurons (**A**, **B**) and in EGFP (open bar), SOD1^{wt} (closed bar), and mutant SOD1 (hatched bars) transfected rat cortical neurons (**C**). Representative kymographs showing FAT of mitochondria in motoneurons are shown (A). Mutant SOD1 did not affect the percentage of motile mitochondria in either motoneurons or transfected cortical neurons (B, C panels a) but disturbed the balance of transport to inhibit anterograde and promote retrograde movement (B, C panels b and c). Statistical significance was determined by one-way ANOVA followed by Newman–Keuls Multiple Comparison Test (ns: not significant, $^{*}P < 0.05$).

time-lapse recordings. The total distances traveled by MBO^{APP} in the presence of mutant SOD1 were significantly less than in the presence of SOD1^{wt} or CAT control (Fig. 2Ba). Examination of retrograde and anterograde movements separately revealed that mutant SOD1 reduced the distances traveled by MBO^{APP} equally in both directions (Fig. 2Bb and c). Thus, mutant SOD1 also inhibits FAT of MBO^{APP} but in contrast to mitochondria, mutant SOD1 damage to MBO^{APP} movement shows no directional selectivity. In summary these data demonstrate that different ALS-linked mutant SOD1 disrupts FAT in similar fashions, but the precise nature of this disruption is cargo-specific.

Increased net retrograde transport of mitochondria correlates with decreases in the activity, velocity and persistence of anterograde mitochondrial motors

Whereas mutant SOD1 inhibited total MBO^{APP} transport, the disturbance of mitochondrial FAT displayed directional selectivity. To gain insight into the mechanism underlying this selectivity, we analyzed the activity of the molecular motors that transport mitochondria by calculating the frequency of anterograde and retrograde transport events in motoneurons. We determined the position of all mitochondria per time point of time-lapse recordings and from this positional information we calculated the number of movement events per mitochondria per minute. To define movement events we applied a velocity threshold of 0.3 μm/s between successive time points. This threshold was set to only include microtubule-based movements since the reported velocity of actin-based transport of mitochondria was well below 0.3 μm/s (18).

In ntg and SOD1^{wt} motoneurons, the overall frequency of movement (anterograde and retrograde combined) was roughly five events per minute per mitochondria (Fig. 3A). Accordingly, mitochondria moved during only 25% of the observation time and were stationary during the remaining 75% of the observation time. The overall level of activity of

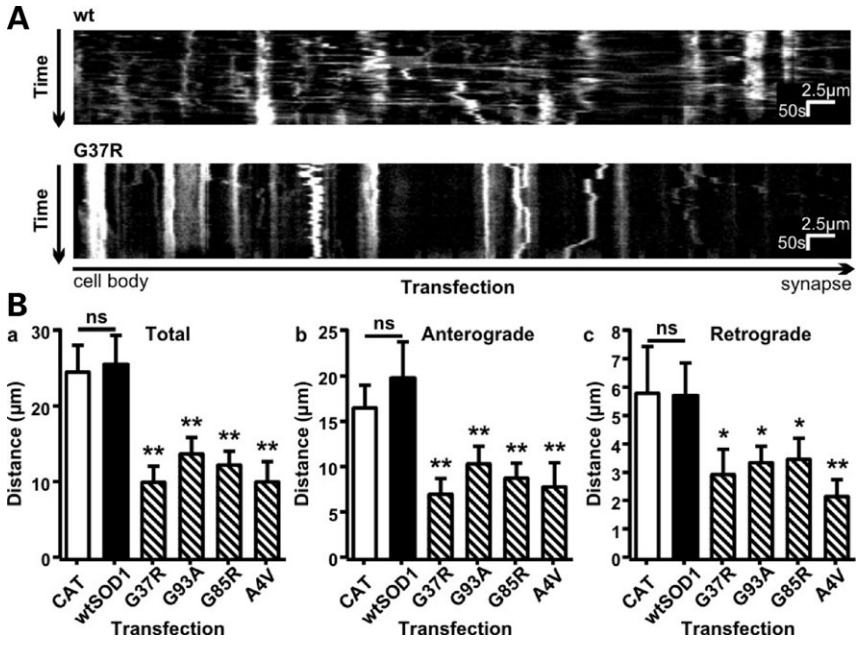

Figure 2. Mutant SOD1 disrupts FAT of MBO^{APP}. Rat cortical neurons were co-transfected with APP-EGFP and vector containing CAT, $SOD1^{wt}$, $SOD1^{G37R}$, $SOD1^{G93A}$, $SOD1^{G85R}$ or $SOD1^{A4V}$. MBO^{APP} FAT was recorded in time-lapse (1–5 s interval, 10 min). Representative kymographs showing transport of MBO^{APP} in $SOD1^{wt}$ and $SOD1^{G37R}$ transfected neurons are shown (**A**). Total transport was quantified as the distance moved per minute of observation time (anterograde and retrograde movements combined; **B**a). The distances that MBO^{APP} moved anterograde (Bb) and retrograde (Bc) were also determined. Total, retrograde and anterograde MBO^{APP} movement were all significantly less in the presence of mutant SOD1s. Statistical significance was determined by one-way ANOVA followed by Newman–Keuls Multiple Comparison Test (ns: not significant, $^{*}P < 0.05$, $^{**}P < 0.01$).

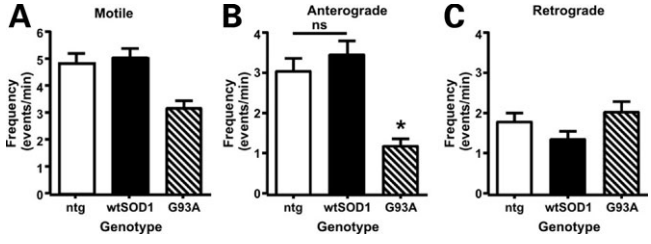

Figure 3. $SOD1^{G93A}$ inhibits anterograde transport activity in motoneurons. FAT of mitochondria was recorded in ntg (open bar), $SOD1^{wt}$ (closed bar), and $SOD1^{G93A}$ (hatched bar) motoneurons. Transport activity was determined as the frequency of all motile events (**A**), and anterograde (**B**) and retrograde events (**C**) separately. $SOD1^{G93A}$ induced a significant decrease in anterograde transport activity (B). Statistical significance was determined by one-way ANOVA (Kruskis–Wallis) followed by Dunn's Multiple Comparison Test (ns: not significant; $^{*}P < 0.05$).

Table 1. $SOD1^{G93A}$ decreases the velocity of anterograde mitochondrial FAT motors

Genotype	Anterograde			Retrograde		
	Velocity (μm/s)	SD	*P*-value	Velocity (μm/s)	SD	*P*-value
ntg	1.00	0.31		0.87	0.22	
$SOD1^{wt}$	1.00	0.13	ns	0.92	0.18	ns
$SOD1^{G93A}$	0.72	0.12	<0.05	0.85	0.16	ns

The velocity was quantified in ntg, $SOD1^{wt}$ and $SOD1^{G93A}$ motoneurons. $SOD1^{G93A}$ induced a significant decrease in the velocity of anterograde movements, but did not affect retrograde velocity. Statistical significance was determined by one-way ANOVA (Kruskal–Wallis) followed by Dunn's Multiple Comparison Test (ns: not significant; *P*-values are indicated; SD: standard deviation).

mitochondrial molecular motors was unchanged in $SOD1^{G93A}$ motoneurons, but the anterograde frequency was decreased by almost 60% while the retrograde frequency remained unchanged (Fig. 3). As a result the retrograde transport activity had become greater than the anterograde transport activity (Fig. 3, $P = 0.036$, Mann–Whitney test), thus explaining the net retrograde transport of mitochondria in $SOD1^{G93A}$ motoneurons.

To examine if $SOD1^{G93A}$ also affected the properties of the molecular motors that transport mitochondria, we next determined the velocity of mitochondrial FAT, the persistence of unidirectional continuous movements, and the duration of pauses in between movements. Whereas the frequency of mitochondrial FAT is an indicator of regulation of mitochondrial transport (activation vs. inactivation), the velocity is an indicator of the ATPase activity and the persistence indicates the active period or process of the motors involved.

The average velocity of anterograde and retrograde mitochondrial transport in ntg motoneurons was 1.00 ± 0.31 μm/s and 0.87 ± 0.13 μm/s, respectively (Table 1), which is higher than in N2A cells and hippocampal neurons but well within the range of reported speeds (18,19). These velocities did not differ significantly in $SOD1^{wt}$ motoneurons but in $SOD1^{G93A}$ neurons, whilst the velocity of retrograde transport was unaffected, the velocity of anterograde transport was significantly decreased (Table 1).

Table 2. $SOD1^{G93A}$ decreases persistence of anterograde mitochondrial FAT motors

Genotype	Anterograde			Retrograde		
	Time (s)	SD	*P*-value	Time (s)	SD	*P*-value
ntg	9.54	15.25		7.18	9.31	
$SOD1^{wt}$	10.24	14.81	ns	6.68	8.12	ns
$SOD1^{G93A}$	5.53	7.29	<0.001	6.89	9.01	ns

The persistence of continuous uni-directional movement was quantified in ntg, $SOD1^{wt}$ and $SOD1^{G93A}$ motoneurons. $SOD1^{G93A}$ induced a significant decrease in the persistence of anterograde movements, but did not affect the persistence of retrograde transport. Statistical significance was determined by one-way ANOVA (Kruskal–Wallis) followed by Dunn's Multiple Comparison Test (ns: not significant; *P*-values are indicated; SD: standard deviation).

Table 3. Duration of stationary periods between movements

Genotype	Time (s)	SD	*P*-value
ntg	62.72	117.1	
$SOD1^{wt}$	62.84	111.9	ns
$SOD1^{G93A}$	72.11	121.3	ns

The duration of stationary periods between movements was quantified in ntg, $SOD1^{wt}$ and $SOD1^{G93A}$ motoneurons. The duration of stationary periods between movements was not significantly affected by $SOD1^{G93A}$. Statistical significance was determined by one-way ANOVA (Kruskal–Wallis) followed by Dunn's Multiple Comparison Test (ns: not significant; *P*-values are indicated; SD: standard deviation).

The persistence of mitochondrial movements in both anterograde and retrograde directions showed no significant differences between ntg and $SOD1^{wt}$ motoneurons and the duration of time that mitochondria remained stationary between movements was also not significantly different in any genotype. However, in $SOD1^{G93A}$ motoneurons, the persistence of movement was significantly reduced in the anterograde but not retrograde directions as compared to controls (Tables 2 and 3). Thus, $SOD1^{G93A}$ inhibited the activity of mitochondrial anterograde motors and affected their properties but did not affect retrograde mitochondrial motors.

Mutant SOD1 causes depletion of mitochondria from the axon and increases inter-mitochondrial distance

The net increase in retrograde moving mitochondria in the presence of mutant SOD1 predicts that they will vacate axons and accumulate in cell bodies. To test this possibility further, we investigated the spatial distribution of mitochondria in $SOD1^{G93A}$ and ntg motoneurons, and in cortical neurons transfected with control vector, wild type or mutant SOD1s. The neurons were fixed and the mitochondria were visualized by immuno-staining of mitochondria-specific Mn superoxide dismutase (MnSOD) or by DsRed-mito expression. We determined mitochondrial density in whole axons by counting the number of mitochondria in defined 50 μm segments and converting these counts to densities (mitochondria/μm). Mitochondria in cell bodies were too abundant to resolve and count; therefore, we quantified the intensity of the mitochondrial fluorescent signal in this compartment. In both motor neurons and transfected cortical neurons, we observed a significant decrease in mitochondria in axons and a corresponding increase in their numbers in cell bodies in presence of mutant SOD1 compared to controls (Fig. 4).

We also analyzed if the distribution of axonal mitochondria was uniform, clustered or random and if mutant SOD1 altered this distribution in any way. In both motoneurons and transfected cortical neurons, the distribution of mitochondria was uniform irrespective of the presence or absence of mutant SOD1 (Supplementary Material, Table S1). However, due to the reduced numbers of axonal mitochondria the inter-mitochondrial distance was significantly increased by 30–50% in the presence of mutant SOD1 (Table 4). Thus, the net increase in retrograde transport of mitochondria induced by mutant SOD1 leads to their accumulation in cell bodies and diminution in axons but a uniform axonal mitochondria spacing is preserved albeit with increased inter-mitochondrial distance.

$SOD1^{G93A}$-induced disruption of FAT correlates with mitochondrial damage

Mutant SOD1 associates with and damages mitochondria, and mitochondrial alterations are found well before initial disease symptoms in mutant SOD1 transgenic mice (20–24). To assess if the mitochondria in the $SOD1^{G93A}$ motoneurons studied here displayed evidence of damage, we quantified the mean CMXROS fluorescence of individual mitochondria in the motoneurons used for analysis of FAT, and also their morphology. CMXROS accumulates in mitochondria based on their negative inner membrane potential that is generated by mitochondrial electron transport activity (25). Hence CMXROS fluorescence correlates with mitochondrial function. Although no differences were detected between ntg and $SOD1^{wt}$ motoneurons, $SOD1^{G93A}$ reduced CMXROS fluorescence by 20% (Table 5). Likewise, morphometric analysis revealed that mitochondria in $SOD1^{G93A}$ motoneurons had a lower aspect ratio as compared to both ntg and $SOD1^{wt}$ neurons (Table 5). Such rounding up has been shown to accompany mitochondrial damage (26). Thus, the alterations to FAT of mitochondria induced by mutant SOD1 correlate with markers for mitochondrial damage.

DISCUSSION

How mutant SOD1 induces selective motoneuron death in ALS is not properly understood. Nevertheless, two prominent features of mutant SOD1 toxicity are damage to slow axonal transport and mitochondria. Disruption to slow axonal transport of the cytoskeleton is one of the earliest pathological events in mutant SOD1 mice (9,10), and mutant SOD1 selectively associates with and damages mitochondria (20–24). Here we have used time-lapse microscopy to quantify for the first time the effects of mutant SOD1 on FAT of bona fide axonal cargoes in living neurons. We analyzed movement of mitochondria and APP; APP has been used previously as a

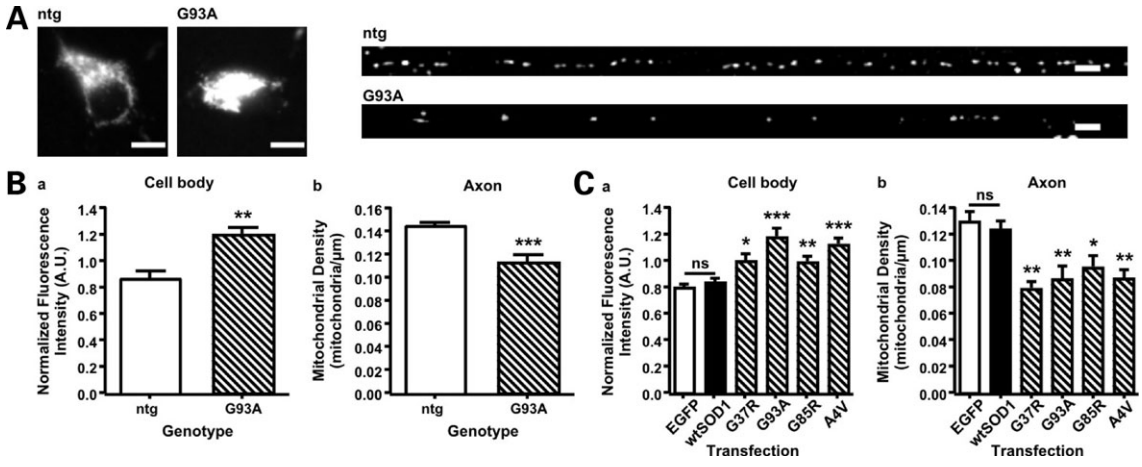

Figure 4. Mutant SOD1 causes depletion of mitochondria from axons. The distribution of mitochondria was analyzed in motoneurons from ntg and SOD1^{G93A} transgenic mice, and in rat cortical neurons transfected with controls or mutant SOD1. (**A**) Shows representative examples of mitochondria immuno-stained for MnSOD in the cell body and axon (proximal 300 μm) of ntg and SOD1^{G93A} transgenic motoneurons (scale bar = 10 μm). To evaluate the number of mitochondria in the cell body, the mean fluorescence intensity of MnSOD staining or DsRed1-mito was determined. Mitochondrial density in axons was determined by counting the numbers of mitochondria in 50 μm segments commencing at the axon hillock, and converting these to mitochondrial density (mitochondria/μm). Mutant SOD1 induced a significant increase in mitochondria in cell bodies of both motoneurons (**B**a) and rat cortical neurons (**C**a) and a corresponding decrease in axonal mitochondria in both cell types (Bb, Cb). Statistical significance was determined by *t*-test (motoneurons) or one-way ANOVA followed by Newman–Keuls Multiple Comparison Test (cortical neurons) ($^{*}P < 0.05$, $^{**}P < 0.01$ and $^{***}P < 0.001$).

Table 4. ALS mutant SOD1 increases the inter-mitochondrial distance in axons

	Distance (μm)	SD	*P*-value
A. *Motoneurons*			
Genotype			
ntg	6.86	0.54	
SOD1^{G93A}	9.04	2.14	<0.001
B. *Cortical neurons*			
Transfection			
EGFP	7.20	1.32	
EGFP-SOD1^{wt}	7.63	1.02	ns
EGFP-SOD1^{G37R}	11.51	2.36	<0.01 (versus EGFP) <0.05 (versus SOD1^{wt})
EGFP-SOD1^{G93A}	10.83	2.05	<0.05
EGFP-SOD1^{G85R}	12.09	4.90	<0.05
EGFP-SOD1^{A4V}	11.41	4.18	<0.05

The inter-mitochondrial distance was calculated as the distance between the centers of adjacent axonal mitochondria. ALS mutant SOD1 caused a significant increase in inter-mitochondrial distance in both transgenic motoneurons and transfected cortical neurons. Statistical significance was determined by unpaired *t*-test or one-way ANOVA followed by Newman–Keuls Multiple Comparison Test (ns: not significant; *P*-values are indicated; SD: standard deviation).

Table 5. ALS mutant SOD1 damages mitochondria

	A. CMXROS uptake (mitochondrial membrane potential)			B. Aspect ratio		
Genotype	Fluorescence intensity	SD	*P*-value	Aspect ratio	SD	*P*-value
ntg	1.09	0.34		2.23	1.01	
SOD1^{wt}	1.08	0.18	ns	2.56	1.31	ns
SOD1^{G93A}	0.84	0.45	<0.001	1.94	0.86	<0.001

Mitochondrial function was determined by measurement of CMXROS uptake (A) and aspect ratio of mitochondria (B). SOD1^{G93A} significantly reduced both CMXROS uptake and aspect ratio, indicating reduced mitochondrial function in SOD1^{G93A} motoneurons. Statistical significance was determined by one-way ANOVA (Kruskal–Wallis) followed by Dunn's Multiple Comparison Test (ns: not significant; *P*-values are indicated; SD: standard deviation).

marker for FAT of MBOs (12–16). We demonstrate that mutant SOD1 perturbs FAT of both cargoes but that the precise nature of this damage is different for each cargo. Whereas mutant SOD1 inhibited anterograde but not retrograde mitochondrial transport, both anterograde and retrograde transport of MBO^{APP} were reduced to a similar extent.

The mechanisms underlying the differential effect of mutant SOD1 on FAT of mitochondria and MBO^{APP} are not clear. Both mitochondria and MBOs are transported along microtubules by kinesin and dynein molecular motors but the precise mechanisms that regulate these motors and the details of their attachment to cargoes are still poorly understood. Recently, Milton (also known as GRIF-1/OIP106/TRAK1/2) and Miro have been identified as adaptor proteins that connect mitochondria to kinesin heavy chains but how they might be involved in the regulation of transport is unclear (27,28). Several groups have demonstrated that p38 stress-activated kinase is activated in mutant SOD1 transgenic mice (29–33) and p38 (and other members of the stress-activated protein kinase family) has been implicated in the regulation of FAT (34,35). Finally, mutant SOD1 has been shown to associate with components of the dynein complex responsible for retrograde axonal transport although whether this influences dynein function is again not known (36). Whatever the precise mechanisms are, our detailed analyses of mitochondrial FAT clearly identify that the mitochondrial anterograde transport machinery is a specific target of mutant SOD1, and that mutant SOD1 disturbs FAT by targeting regulatory pathways as well as by damaging the motors involved.

Interestingly, damaging mitochondria with the electron transport inhibitor antimycin also causes an increase in their retrograde movements (3). Mutant SOD1 associates with and damages mitochondria (20–24) and we demonstrate that mitochondria in the $SOD1^{G93A}$ motoneurons studied here also show evidence of damage; their membrane potential is reduced and they round up. Thus, the known association of mutant SOD1 with mitochondria and the damage that this induces might act similarly to antimycin to somehow inhibit anterograde transport of mitochondria.

The altered transport of mitochondria led to their redistribution in neurons with fewer mitochondria in axons and more in cell bodies. Accumulation of mitochondria in cell bodies and proximal axons is a reported feature in $SOD1^{G93A}$ transgenic mice and in ALS patients (37,38). The subcellular distribution of mitochondria is an important component of their function; they localize in neurons to regions of high energy demand such as cell bodies (where most protein synthesis occurs) and nodes of Ranvier (4). Interestingly, despite the diminution of axonal mitochondria in mutant SOD1 expressing neurons, their uniform spacing was preserved. This suggests that the mechanisms that regulate the spatial distribution of axonal mitochondria are independent of the mechanisms that regulate their delivery to the axonal compartment and that mutant SOD1 affects the latter but not the former. Nonetheless, as a consequence of this redistribution, in mutant SOD1 neurons one mitochondrion serves an axonal segment of almost twice the size of that in control cells. In addition to mitochondrial dysfunction, this is likely to enhance axonal stress by further limitation of the local availability of mitochondrial metabolites and ATP, and by reducing Ca^{++} buffering capacity. Indeed, motor neurons have particularly low Ca^{++} buffering capacity (39). Such a thinning of mitochondria may also reduce ATP supply to kinesin and dynein motors in axons and this may contribute to the non-directional reduction of MBO^{APP} transport observed here. Mitochondrial movement would be exempted since they carry their own energy supply.

Further investigations are necessary to unravel the molecular events leading to disturbed FAT in ALS. However, our data clearly reveal the anterograde mitochondrial transport machinery is a specific target of mutant SOD1 toxicity and that altered FAT involving damage to mitochondria is one of the earliest pathological events associated with mutant SOD1. As such, correcting FAT defects represent a promising therapeutic target.

MATERIALS AND METHODS

Plasmids

ALS mutant human SOD1 were generated using a Chameleon mutagenesis kit (Stratagene, Amsterdam, The Netherlands), and cloned into pCIneo (Promega, Southhampton, UK) or pEGFP-C2 (Clontech, Basingstoke, UK) to create N-terminal EGFP-tagged versions. Human APP (isoform 695) was created by cloning into plasmid pEGFP-N1 (Clontech) following mutation of the stop codon. Vector pDsRed-mito was from Clontech.

Cell culture and transfections

$SOD1^{wt}$ [B6SJL-TgN(SOD1)2Gur] and $SOD1^{G93A}$ [B6SJL-TgN (SOD1-G93A)1Gur] transgenic mice were obtained from the Jackson Laboratory (Bar Harbor, ME) and were back-crossed to C57BL/6 for >20 generations. Genotyping of embryos was performed according to the protocol provided by the Jackson Laboratory. Primary motoneurons were cultured from E13.5 $SOD1^{G93A}$ or $SOD1^{wt}$ mouse embryos and their ntg littermates as described previously (11), and were plated on poly-D-ornithine (1.5 μg/ml; Sigma, Poole, UK) and laminin (3 μg/ml; Sigma) coated coverslips at 40 000 cells per coverslip in Neurobasal medium supplemented with 1% B27, 2% horse serum, 50 μg/ml streptomycin, 50 U/ml penicillin, 0.5 mM L-glutamine, 25 μM glutamic acid (all from Invitrogen, Paisley, UK), 25 μM 2-mercaptoethanol (Sigma), 10 ng/ml CNTF, and 100 pg/ml GDNF (both from R&D Systems, Abingdon, UK). Motoneuron mitochondria were stained for 3 min at 37°C with 66 nM MitoTracker CMXROS (Invitrogen) in fresh culture medium.

Rat cortical neurons were obtained from E18 Wistar rat embryos (Charles River Laboratories, Wilmington, MA) as previously described (40).

For analysis of mitochondrial FAT, rat cortical neurons were co-transfected at DIV5 with 3 μg pDsRed-mito to label mitochondria and 7 μg EGFP, or EGFP-SOD1 using calcium phosphate precipitation as described (40). For analysis of MBO^{APP} FAT, neurons were transfected using Lipofectamine 2000 (Invitrogen). All cortical neurons were used for experiments 36–48 h after transfection.

Immunofluorescence

Motoneurons were fixed for 20 min in 3.7% formaldehyde in phosphate buffered saline (PBS). Following washing and quenching in 50 mM NH_4Cl in PBS for 15 min, the cells were permeabilized in 0.2% Triton X-100 in PBS for 10 min. After blocking for 1 h in 4% fetal calf serum (FCS; Invitrogen) in PBS (FCS/PBS), the cells were incubated for 1 h with rabbit anti-MnSOD (Stressgen, Ann Arbor, MI; 1:100 in FCS/PBS) followed by 1 h incubation with Alexa 568 goat anti-rabbit IgG (Invitrogen, 1:1000 in FCS/PBS). Between each step the cells were washed three times in 0.2% Tween20 in PBS.

Microscopy

Live microscopy of mitochondria was performed with an Axiovert 200 microscope (Carl Zeiss Ltd., Welwyn Garden City, UK) equipped with a Polychrome IV monochromator (Till Photonics, Gräfelfing, Germany), EGFP/DsRed filterset (Chroma Technology Corp., Rockingham, VT), 40× EC Plan-Neofluar® N.A. 1.3 objective (Zeiss), Lambda 10-2 filter wheel (Sutter Instrument Company, Novato, CA), and Hamamatsu C4880-80 CCD (Hamamatsu Photonics, Welwyn Garden City, UK). The cells were maintained at 37°C in a custom closed observation chamber using an objective heater (IntraCell, Royston, UK) and mitochondrial movements were recorded for 10–20 min with 3 s time-lapse interval using Openlab software (Improvision, Coventry, UK).

APP-EGFP transport was observed using a Zeiss Axiovert S100 microscope and 100× Plan-Neofluar® N.A. 1.3 objective (Zeiss). Cells were maintained at 37°C under a 5% CO_2 atmosphere using an Open Perfusion Micro-Incubator (Medical Systems Corporation, Greenville, NY). MBO^{APP} movements were recorded for 10 min with 5 s time-lapse interval using a Micromax CCD camera (Princeton Instruments, Lurgan, UK) and Metamorph (Molecular Devices Ltd., Wokingham, UK).

For the analysis of mitochondrial distribution, fixed motoneurons were imaged using a 25× LCI Plan-Neofluar® objective (Zeiss) on the Axiovert 200 setup described above.

Image analysis

Image analysis was performed with ImageJ developed by Wayne Rasband (NIH, Bethesda, USA; http://rsb.info.nih.gov/ij/) extended with custom plug-ins (41), or Metamorph. Further calculations and statistical analysis were performed using Excel (Microsoft Corporation, Redmond, WA), and Prism software (GraphPad Software Inc., San Diego, CA).

A custom ImageJ plug-in (available from KJDV) was used to track mitochondria through the time-lapse recordings. Calculations of mitochondrial transport parameters were as described before (19,42) except overall transport of mitochondria was analyzed by calculating the distance between the position of individual mitochondria at the start and end of time-lapse recordings and dividing by the time elapsed. This yielded an overall velocity of transport for all mitochondria that includes anterograde and retrograde movements and stationary periods. Mitochondria were subsequently classified as motile (velocity > 0.1 μm/s) or stationary (velocity ≤ 0.1 μm/s).

APP-EGFP transport was tracked using MetaMorph. Moving MBO^{APP} were defined as those that exhibited movement ≥ 0.3 μm in 5 s; pauses in moving structures were thus defined as any movement < 0.3 μm in 5 s.

Analysis of mitochondrial distribution and function

The spatial distribution of mitochondria within axons was evaluated as described (3). To analyze mitochondrial density, axons were divided in 50 μm segments; the number of mitochondria was counted in each segment, and converted to densities (mitochondria/μm). The inter-mitochondrial distance was determined by computing the distance between the centroids of adjacent mitochondria. The mean CMXROS fluorescence and aspect ratio of mitochondria was measured by determining the mean fluorescence and bounding ellipse for each mitochondrion using the particle analysis function of ImageJ. Aspect ratio was determined by dividing the major and minor axis of the bounding ellipse (26). Mean CMXROS fluorescence was normalized by dividing each value by the average value of all mitochondria of all cells (irrespective of genotype) measured.

Statistics

All data shown comes from at least six cells measured in at least three independent experiments. Statistical methods are detailed in the text.

SUPPLEMENTARY MATERIAL

Supplementary Material is available at HMG Online.

ACKNOWLEDGEMENTS

We thank Dr Liz Smythe for careful reading of the manuscript and helpful discussions.

Conflict of Interest statement. The authors declare no conflict of interest.

FUNDING

This work was supported by grants to CCJM (MRC, Wellcome Trust, European Union VIth Framework NeuroNE, MNDA), AJG (BBSRC, ALSA, MRC) and KJDV (ALSA).

REFERENCES

1. Miller, C.C.J., Ackerley, S., Brownlees, J., Grierson, A.J., Jacobsen, N.J.O. and Thornhill, P. (2002) Axonal transport of neurofilaments in normal and disease states. *Cell Mol. Life Sci.*, **59**, 323–330.
2. Hirokawa, N. and Takemura, R. (2004) Molecular motors in neuronal development, intracellular transport and diseases. *Curr. Opin. Neurobiol.*, **14**, 564–573.
3. Miller, K.E. and Sheetz, M.P. (2004) Axonal mitochondrial transport and potential are correlated. *J. Cell Sci.*, **117**, 2791–2804.
4. Hollenbeck, P.J. and Saxton, W.M. (2005) The axonal transport of mitochondria. *J. Cell Sci.*, **118**, 5411–5419.
5. Duncan, J.E. and Goldstein, L.S. (2006) The genetics of axonal transport and axonal transport disorders. *PLoS Genet.*, **2**, e124.
6. Chevalier-Larsen, E. and Holzbaur, E.L. (2006) Axonal transport and neurodegenerative disease. *BBA-Mol. Basis Dis.*, **1762**, 1094–1108.
7. Boillee, S., Vande Velde, C. and Cleveland, D.W. (2006) ALS: a disease of motor neurons and their nonneuronal neighbors. *Neuron*, **52**, 39–59.
8. Shaw, P.J. (2005) Molecular and cellular pathways of neurodegeneration in motor neurone disease. *J. Neurol. Neurosurg. Psychiatry*, **76**, 1046–1057.
9. Williamson, T.L. and Cleveland, D.W. (1999) Slowing of axonal transport is a very early event in the toxicity of ALS-linked SOD1 mutants to motor neurons. *Nature Neurosci.*, **2**, 50–56.
10. Zhang, B., Tu, P., Abtahian, F., Trojanowski, J.Q. and Lee, V.M. (1997) Neurofilaments and orthograde transport are reduced in ventral root axons of transgenic mice that express human SOD1 with a G93A mutation. *J. Cell Biol.*, **139**, 1307–1315.
11. Kieran, D., Hafezparast, M., Bohnert, S., Dick, J.R., Martin, J., Schiavo, G., Fisher, E.M. and Greensmith, L. (2005) A mutation in dynein rescues axonal transport defects and extends the life span of ALS mice. *J. Cell Biol.*, **169**, 561–567.
12. Goldsbury, C., Mocanu, M.M., Thies, E., Kaether, C., Haass, C., Keller, P., Biernat, J., Mandelkow, E. and Mandelkow, E.M. (2006) Inhibition of APP trafficking by tau protein does not increase the generation of amyloid-beta peptides. *Traffic*, **7**, 873–888.
13. Sisodia, S.S., Koo, E.H., Hoffman, P.N., Perry, G. and Price, D.L. (1993) Identification and transport of full-length amyloid precursor proteins in rat peripheral nervous system. *J. Neurosci.*, **13**, 3136–3142.
14. Kaether, C., Skehel, P. and Dotti, C.G. (2000) Axonal membrane proteins are transported in distinct carriers: a two-color video microscopy study in cultured hippocampal neurons. *Mol. Biol. Cell*, **11**, 1213–1224.
15. Koo, E.H., Sisodia, S.S., Archer, D.R., Martin, L.J., Weidemann, A., Beyreuther, K., Fischer, P., Masters, C.L. and Price, D.L. (1990) Precursor of amyloid protein in Alzheimer disease undergoes fast anterograde axonal transport. *Proc. Natl. Acad. Sci. USA*, **87**, 1561–1565.
16. Stamer, K., Vogel, R., Thies, E., Mandelkow, E. and Mandelkow, E.M. (2002) Tau blocks traffic of organelles, neurofilaments, and APP vesicles in neurons and enhances oxidative stress. *J. Cell Biol.*, **156**, 1051–1063.

17. Ratovitski, T., Corson, L.B., Strain, J., Wong, P., Cleveland, D.W., Culotta, V.C. and Borchelt, D.R. (1999) Variation in the biochemical/biophysical properties of mutant superoxide dismutase 1 enzymes and the rate of disease progression in familial amyotrophic lateral sclerosis kindreds. *Hum. Mol. Genet.*, **8**, 1451–1460.
18. Morris, R.L. and Hollenbeck, P.J. (1995) Axonal transport of mitochondria along microtubules and F-actin in living vertebrate neurons. *J Cell Biol*, **131**, 1315–1326.
19. De Vos, K.J., Sable, J., Miller, K.E. and Sheetz, M.P. (2003) Expression of phosphatidylinositol (4,5) bisphosphate-specific pleckstrin homology domains alters direction but not the level of axonal transport of mitochondria. *Mol. Biol. Cell*, **14**, 3636–3649.
20. Higgins, C.M.J., Jung, C.W., Ding, H.L. and Xu, Z.S. (2002) Mutant Cu, Zn superoxide dismutase that causes motoneuron degeneration is present in mitochondria in the CNS. *J. Neurosci.*, **22**, RC215 (1–6).
21. Ferri, A., Cozzolino, M., Crosio, C., Nencini, M., Casciati, A., Gralla, E.B., Rotilio, G., Valentine, J.S. and Carri, M.T. (2006) Familial ALS-superoxide dismutases associate with mitochondria and shift their redox potentials. *Proc. Natl. Acad. Sci. USA*, **103**, 13860–13865.
22. Mattiazzi, M., D'Aurelio, M., Gajewski, C.D., Martushova, K., Kiaei, M., Beal, M.F. and Manfredi, G. (2002) Mutated human SOD1 causes dysfunction of oxidative phosphorylation in mitochondria of transgenic mice. *J. Biol. Chem.*, **277**, 29626–29633.
23. Pasinelli, P., Belford, M.E., Lennon, N., Bacskai, B.J., Hyman, B.T., Trotti, D. and Brown, R.H., Jr (2004) Amyotrophic lateral sclerosis-associated SOD1 mutant proteins bind and aggregate with Bcl-2 in spinal cord mitochondria. *Neuron*, **43**, 19–30.
24. Liu, J., Lillo, C., Jonsson, P.A., Vande Velde, C., Ward, C.M., Miller, T.M., Subramaniam, J.R., Rothstein, J.D., Marklund, S., Andersen, P.M. *et al.* (2004) Toxicity of familial ALS-linked SOD1 mutants from selective recruitment to spinal mitochondria. *Neuron*, **43**, 5–17.
25. Macho, A., Decaudin, D., Castedo, M., Hirsch, T., Susin, S.A., Zamzami, N. and Kroemer, G. (1996) Chloromethyl-X-Rosamine is an aldehyde-fixable potential-sensitive fluorochrome for the detection of early apoptosis. *Cytometry*, **25**, 333–340.
26. De Vos, K.J., Allan, V.J., Grierson, A.J. and Sheetz, M.P. (2005) Mitochondrial function and actin regulate dynamin-related protein 1-dependent mitochondrial fission. *Curr. Biol.*, **15**, 678–683.
27. Fransson, S., Ruusala, A. and Aspenstrom, P. (2006) The atypical Rho GTPases Miro-1 and Miro-2 have essential roles in mitochondrial trafficking. *Biochem. Biophys. Res. Commun.*, **344**, 500–510.
28. Glater, E.E., Megeath, L.J., Stowers, R.S. and Schwarz, T.L. (2006) Axonal transport of mitochondria requires milton to recruit kinesin heavy chain and is light chain independent. *J. Cell Biol.*, **173**, 545–557.
29. Hu, J.H., Chernoff, K., Pelech, S. and Krieger, C. (2003) Protein kinase and protein phosphatase expression in the central nervous system of G93A mSOD over-expressing mice. *J. Neurochem.*, **85**, 422–431.
30. Wengenack, T.M., Holasek, S.S., Montano, C.M., Gregor, D., Curran, G.L. and Poduslo, J.F. (2004) Activation of programmed cell death markers in ventral horn motor neurons during early presymptomatic stages of amyotrophic lateral sclerosis in a transgenic mouse model. *Brain Res.*, **1027**, 73–86.
31. Tortarolo, M., Veglianese, P., Calvaresi, N., Botturi, A., Rossi, C., Giorgini, A., Migheli, A. and Bendotti, C. (2003) Persistent activation of p38 mitogen-activated protein kinase in a mouse model of familial amyotrophic lateral sclerosis correlates with disease progression. *Mol. Cell Neurosci.*, **23**, 180–192.
32. Ackerley, S., Grierson, A.J., Banner, S., Perkinton, M.S., Brownlees, J., Byers, H.L., Ward, M., Thornhill, P., Hussain, K., Waby, J.S. *et al.* (2004) p38a stress-activated protein kinase phosphorylates neurofilaments and is associated with neurofilament pathology in amyotrophic lateral sclerosis. *Mol. Cell Neurosci.*, **26**, 354–364.
33. Raoul, C., Estevez, A.G., Nishimune, H., Cleveland, D.W., deLapeyriere, O., Henderson, C.E., Haase, G. and Pettmann, B. (2002) Motoneuron death triggered by a specific pathway downstream of Fas: potentiation by ALS-linked SOD1 mutations. *Neuron*, **35**, 1067–1083.
34. Morfini, G., Pigino, G., Szebenyi, G., You, Y., Pollema, S. and Brady, S.T. (2006) JNK mediates pathogenic effects of polyglutamine-expanded androgen receptor on fast axonal transport. *Nat. Neurosci.*, **9**, 907–916.
35. De Vos, K., Severin, F., Van Herreweghe, F., Vancompernolle, K., Goossens, V., Hyman, A. and Grooten, J. (2000) Tumor necrosis factor induces hyperphosphorylation of kinesin light chain and inhibits kinesin-mediated transport of mitochondria. *J. Cell Biol.*, **149**, 1207–1214.
36. Zhang, F., Strom, A.L., Fukada, K., Lee, S., Hayward, L.J. and Zhu, H. (2007) Interaction between familial ALS-linked SOD1 mutants and the dynein complex: Implications of retrograde axonal transport in ALS. *J. Biol. Chem.*, **282**, 16691–16699.
37. Sasaki, S. and Iwata, M. (1996) Impairment of fast axonal transport in the proximal axons of anterior horn neurons in amyotrophic lateral sclerosis. *Neurology*, **47**, 535–540.
38. Sasaki, S. and Iwata, M. (2007) Mitochondrial alterations in the spinal cord of patients with sporadic amyotrophic lateral sclerosis. *J. Neuropath. Exp. Neur.*, **66**, 10–16.
39. Van Den Bosch, L., Van Damme, P., Bogaert, E. and Robberecht, W. (2006) The role of excitotoxicity in the pathogenesis of amyotrophic lateral sclerosis. *BBA-Mol. Basis Dis.*, **1762**, 1068–1082.
40. Ackerley, S., Grierson, A.J., Brownlees, J., Thornhill, P., Anderton, B.H., Leigh, P.N., Shaw, C.E. and Miller, C.C. (2000) Glutamate slows axonal transport of neurofilaments in transfected neurons. *J. Cell Biol.*, **150**, 165–176.
41. Abramoff, M.D., MagalHaes, P.J. and Ram, S.J. (2004) Image Processing with ImageJ. *Biophotonics Int.*, **11**, 36–42.
42. De Vos, K.J. and Sheetz, M.P. (2007) Visualization and quantification of mitochondrial dynamics in living animal cells. *Methods Cell Biol.*, **80**, 627–682.